

Electronic states of Mn impurities and magnetic coupling between Mn spins in diluted magnetic semiconductors

W. H. Wang,^{1,2} Liang-Jian Zou,¹ and Y. Q. Wang¹

¹Key Laboratory of Materials Physics, Institute of Solid State Physics, Chinese Academy of Sciences,
P. O. Box 1129, Hefei 230031, China

²Graduate School of the Chinese Academy of Sciences, Hefei 230031, China

(Received 7 December 2004; revised manuscript received 20 June 2005; published 8 November 2005)

Electronic states of single Mn impurities and magnetic couplings between Mn spins in diluted magnetic semiconductors have been studied systematically. It has been clearly shown that in the ground state, Mn spin antiferromagnetically (AFM) couples to surrounding As(N) when p - d hybridization V_{pd} is large and both the hole level E_v and the impurity level E_d are close to the middle of the gap; or very weak ferromagnetically (FM) when V_{pd} is small and both E_v and E_d are deep in the valence band. The Mn spin couplings are Heisenberg AFM for half-filled hole orbits; on the contrary, the couplings between Mn spins are double-exchange-like FM when the hole occupation in the p orbits is away from half-filling, and this accounts for the FM order in III-V semiconductors. The important role of the antisite As(N) compensation or the hole phase separation for the stability of FM ground state in wide-gap diluted magnetic semiconductors is emphasized.

DOI: 10.1103/PhysRevB.72.195202

PACS number(s): 75.50.Pp, 75.10.-b

I. INTRODUCTION

Diluted magnetic semiconductors (DMS), such as $\text{Ga}_{1-x}\text{Mn}_x\text{As}$ and $\text{Ga}_{1-x}\text{Mn}_x\text{N}$, with ferromagnetic (FM) Curie temperature (T_c) as high as 110 K in $\text{Ga}_{1-x}\text{Mn}_x\text{As}$, or even as room temperature in $\text{Ga}_{1-x}\text{Mn}_x\text{N}$ have attracted much attention, since these compounds provide perspective applications in the fabrication of spintronics devices as well as in quantum computers.¹⁻⁵ The unusually high FM Curie temperatures in Mn-doped or Cr-doped III-V semiconductors with such low concentrated magnetic ions and the interesting magnetotransport properties have also raised many fundamental problems, e.g., the electronic states of $3d$ impurities and the origin of the FM long-range order²⁻⁴ (LRO). Many experiments have established the fact that local magnetic moments \mathbf{S} and hole states are simultaneously introduced in DMS as galliums are substituted by manganese. An elaborate relationship between the Mn concentration and the Curie point T_c in Ref. 1 and lots of other experiments^{6,7} demonstrated the important role of mobile hole carriers in the formation of FMLRO in DMS, suggesting that the FM coupling between Mn spins is mediated through these delocalized holes.

Some microscopic mechanisms have been proposed to explain the microscopic origin of the carrier-induced⁸⁻¹² FMLRO in DMS. The coexistence of local magnetic moments at the Mn site and mobile carriers at surrounding As(N) sites suggests that the Ruderman-Kittel-Kasuya-Yosida (RKKY) interaction between Mn spins is a natural candidate to account for the origin of FMLRO in III-V semiconductors. Dietl *et al.*⁸ interpreted the magnetic properties of $\text{Ga}_{1-x}\text{Mn}_x\text{As}$ in terms of the RKKY interaction and Zener scenario within the mean-field approximation. Although this theory successfully explained the dependence of the Curie temperature T_c and the spontaneous magnetization on the doping concentration in some doping range,⁹ there are still some important issues to be clarified. First of all, the mean-

field RKKY theory is valid only when isolated local spins are merged in the sea of highly degenerate carriers, i.e., local spin density N_s is much less than carrier density n_h , and the carrier bandwidth D is much greater than the spin-hole exchange constant J . However, in DMS, the hole density, $n_h \ll N_s$, and the Mn-As(N) spin-hole exchange constant, $J \approx 1$ eV, is much larger than the Fermi energy, $E_F \approx 0.3$ eV, of the hole carriers.¹³ Second, an updated experiment has clearly shown that in $\text{Ga}_{1-x}\text{Mn}_x\text{As}$, the holes are bound to Mn acceptors¹⁴⁻¹⁶ and form an impurity band in the heavy doping regime, rather than a degenerate wide conduction band. Furthermore, the averaged Mn coordinate number z is less than that of the conventional three-dimensional ferromagnets, thus it is expected that there will be a large discrepancy between the mean-field result and the realistic situation. Therefore, the mean-field RKKY or Zener⁸ theory might not be accurate for describing the FM ordering³ in DMS.

The double-exchange model, which is responsible for the FM order in doped perovskite manganites, was also suggested for the FM coupling of distant Mn spins in DMS theoretically and experimentally.^{3,10,11} Based on the first-principles calculation, Akai found in $(\text{In},\text{Mn})\text{As}$,³ the carriers are d character and the FM state is half-metallic, an analogy with doped manganites, so he suggested the double-exchange interaction stabilizes the FM ground-state (GS) in $(\text{In},\text{Mn})\text{As}$. However, there exist lots of difference between DMS and manganites: the spatial separation of Mn spins in DMS is much further than that of dense Mn spins in manganites; the direct hopping integral between d electrons is very small in Mn-doped GaAs, and the valence fluctuation in Mn $3d$ orbits is small, dissimilar to the mixed valence of $3d^3$ and $3d^4$ in doped manganites. It is well known that in double-exchange manganites, the magnetic coupling between two nearest-neighbor Mn spins approximately behaves as $|\cos(\theta/2)|$; here θ is the azimuthal angle of two spins. To date, this behavior has not been explicitly confirmed in DMS experimentally. Also the polaronic mediated FM

mechanism¹² and some other theories^{17–19} are also proposed to interpret the origin of FMLRO. Several debated theories indicate that more efforts are needed for the microscopic origin of the FM order in DMS.

One of the central problems in DMS is to understand the electronic state properties of the impurities and the magnetic interaction of manganese spins, especially their evolution with various physical parameters and the doping concentration of DMS. These electronic properties are essential for our understanding of the microscopic mechanism of FMLRO in DMS. Earlier studies by Zunger and Lindefelt,^{20,21} Delerue *et al.*²² and some other authors^{23,24} on the electronic structures of single Mn and other transition-metal impurity III-V and IV semiconductors provided much valuable information. Based on local density approximation and unconstrained mean-field approximation, Zunger and Lindefelt,^{20,21} studied the chemical trends of the effective crystalline fields, the energy levels, and the density of states (DOS) of the transition-metal impurities. The substitutional impurity state properties of different transition-metal atoms in III-V semiconductors were also analytically studied in Ref. 22 to explore the dependence of the impurity energy levels on the nuclei charges of the transition-metal atoms. More recently the FM GS in Mn-doped DMS has been confirmed by a lot of authors based on the first-principles electronic structure calculations, for example, see Refs. 23 and 24. However, it is not well understood the nature of the couplings between Mn spins, the evolution of the magnetic couplings between Mn spins with the doping concentration, the p - d hybridization strength, the energy gap of the host III-V semiconductors, and the energy levels of the $3d$ impurities and of the $4p$ holes, etc. These factors are crucial for our understanding the FM ordering and the unusual transport in DMS.

The aim of this paper is to elucidate the electronic states and the magnetic properties of a single Mn–As(N) cluster and the spin couplings between two Mn–As(N) clusters for various parameters. We find that in DMS, the azimuthal angle dependence of the magnetic coupling energy between two Mn spins is proportional to $|\cos(\theta/2)|$, indicating that the FM origin in DMS is double-exchange-like. In the rest of this paper, after describing the model Hamiltonian in Sec. II, we first study the GS of single Mn–As(N) clusters for various electron configurations, determining the parameter range of the antiferromagnetic (AFM) coupling in the single Mn–As(N) cluster in Sec. III A; then in Sec. III B, we present the Mn–Mn spin couplings in the GS of two Mn–As(N) clusters and show that the FM coupling is double-exchange-like for the hole occupation away from the half-filling, or Heisenberg-like AFM for the half-filling, and the compensation of antisite defects to the substitutions or the inhomogeneity of the hole distribution (electron phase separation) plays crucial roles for stable FM ground state in DMS. Section IV is devoted to the remarks and conclusions.

II. MODEL HAMILTONIAN

As manganese substitute the host atoms In, Ga, or Al in III-V semiconductors, such as InAs, GaAs, GaN, or AlN, we now have a basic interaction scenario in DMS from various

early experimental and theoretical studies: the five valence electrons of As(N) occupy the four sp^3 dangling bonds with symmetry A_1 and T_2 , and the two outer $4s$ electrons of Mn covalently couple to the A_1 orbit of the As or N dangling bonds. The Mn impurity, as an effective mass acceptor, contributes a spin and a hole. The spin localizes in Mn site, while the hole is bound to As or N site around Mn with an extension radius of r_s larger than the lattice constant. The five $3d$ electrons of Mn are separated into an inert local spin S of $3d^4$ configuration and a $3d$ electron which hybridizes with $4p$ orbit, which couple with each other via strong Hund's coupling J_H . The $3d$ electrons interact with the holes in the p orbits of the surrounding As or N sites through the hybridization V_{pd} . Under the T_d symmetry environment of the zinc-blende III-V semiconductors, the hole randomly occupies one of the three T_2 orbits contributed from four nearest-neighbor As or N atoms around the Mn spin. Meanwhile, in the T_d crystalline field, the $3d$ orbits of Mn ions split into lower energy E_g -like d orbits with pure atomic character and almost not coupling to As or N atoms, and higher energy T_{2g} -like orbits coupling to the T_{2p} orbits of As or N atoms.²² Due to the strong Hund's coupling, the $3d$ electron hybridized with holes still interacts with the rest electrons of the local spin $S(S=2)$ of Mn $3d^4$ configuration via Hund's coupling J_H . The on-site Coulomb interactions between $3d$ electrons U_d and between holes U_v are also taken into account. Here, U_v is usually much smaller than U_d .²²

With the increase of Mn concentration, the wave functions of the holes centered at As or N sites with large radius r_s start to overlap with each other. The hopping integral between holes V_h crucially depends on the extension radius r_s and the hole density n_h . Thus the Hamiltonian modeling the preceding physics in DMS reads

$$\hat{H} = \sum_i \hat{H}_0(i) + \hat{H}_1, \quad (1)$$

$$\begin{aligned} \hat{H}_0(i) = & \sum_{\sigma} \left(E_d \hat{d}_{i\sigma}^{\dagger} \hat{d}_{i\sigma} + E_v \hat{c}_{i\sigma}^{\dagger} \hat{c}_{i\sigma} + \frac{U_d}{2} n_{i\sigma}^d n_{i\bar{\sigma}}^d + \frac{U_v}{2} n_{i\sigma}^c n_{i\bar{\sigma}}^c \right) \\ & - \frac{J_H}{2} \sum_{\mu\nu} \mathbf{S}_i \cdot \hat{d}_{i\mu}^{\dagger} \sigma_{i\mu\nu} \hat{d}_{i\nu} + \sum_{\sigma} V_{pd} (\hat{d}_{i\sigma}^{\dagger} \hat{c}_{i\sigma} + \hat{c}_{i\sigma}^{\dagger} \hat{d}_{i\sigma}), \end{aligned} \quad (2)$$

$$\hat{H}_1 = \sum_{\langle ij \rangle \sigma} V_h (\hat{c}_{i\sigma}^{\dagger} \hat{c}_{j\sigma} + \hat{c}_{j\sigma}^{\dagger} \hat{c}_{i\sigma}), \quad (3)$$

where $H_0(i)$ describes the electronic interactions in the i th Mn–As cluster, and H_1 the hopping process between holes. E_d and E_v denote the bare d -electron and p -orbit energy levels, respectively; $\hat{d}_{i\sigma}^{\dagger}$ and $\hat{c}_{i\sigma}^{\dagger}$ are the creation operators of the $3d$ electron and $4p$ electrons with spin σ in the i th Mn–As(N) unit; $n_{i\sigma}^d$ and $n_{i\sigma}^c$ denote the electron occupation number of the hybridized d orbit and p orbit with spin σ , and $n = \sum_{\sigma} (n_{\sigma}^c + n_{\sigma}^d)$ is the total electron number.

Unlike some other authors, this Hamiltonian is not expressed as a simple Kondo lattice model. As we addressed in Sec. I, there exists strong pd hybridization between Mn $3d$

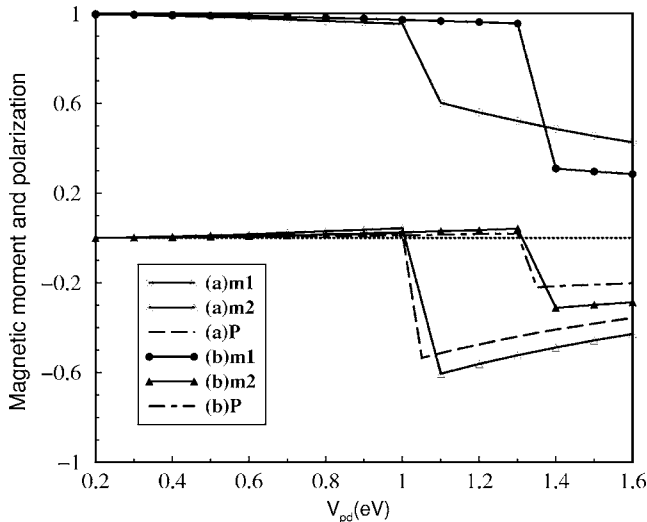


FIG. 1. Hybridization dependence of magnetic moment m_1 of the hybridized d electron and magnetic moment m_2 and spin polarization P of p electrons in the GS of Mn–As(N) cluster for (a) GaAs:Mn, $E_v = -0.95$ eV, $E_d = -1.2$ eV; (b) GaN:Mn, $E_v = -1.8$ eV, $E_d = -0.5$ eV. The other parameters: $U_d = 4.0$ eV, $U_v = 0.35$ eV, $J_H = 1.0$ eV.

orbitals and As or N p orbitals, so the $3d$ electron occupation varies with the pd hybridization and the total Mn spins are not completely localized. In the present scenario, the p holes are bound near Mn sites or extend only over a few of lattice constants, forming an impurity band with very narrow bandwidth. So the Kondo lattice model is not proper in describing the physics in DMS. In this paper, the p and d levels, E_v and E_d , are taken with respect to the middle of the band gap.

III. THEORETICAL RESULTS

In the following, we present first the electronic states of a single Mn impurity and its evolution with the interaction parameters in a single Mn–As cluster, and then the effective couplings between Mn spins of two Mn–As clusters in the DMS background.

A. Single Mn impurity

We study the electronic states of a cluster with a Mn impurity and its ligand As or N, which describes the situation that the distance of Mn ions is so far that the Mn–Mn interaction can be neglected and $V_h = 0$, thus no summation over the lattice is needed in Eqs. (1)–(3). The local spin \mathbf{S} is assumed to be aligned in the z axis. The electronic states and the magnetic properties of the Mn–As cluster are easily obtained by the exact diagonalization to H_0 for various physical parameters and electron configurations. In contrast to the local moments formation in the Anderson impurity model, the p electron is AFM polarized with respect to the local spin as the p – d hybridization V_{pd} is stronger than a critical value V_c , as seen in Fig. 1. When $V_{pd} < V_c$, we find that the p orbit is almost fulfilled in the GS and the polarization of the electrons in the p orbit is positive and very weak. The p and d electron occupations are almost fixed with the increase of

V_{pd} . A very small fraction of spin-down p electron transfers to the $3d$ orbit, and the magnetic moment of the hybridized $3d$ orbit deviates from $1\mu_B$ very little, which leads to the weak and positive polarization of the p orbit and $S \approx 5/2$ at Mn site. The maximum of the polarized moment of each As or N is about $0.023\mu_B$ in the Mn–As cluster or $0.021\mu_B$ in the Mn–N cluster as $V_{pd} \rightarrow V_c$.

As V_{pd} becomes larger than $V_c \approx 1.0$ eV in the Mn–As cluster or $V_c \approx 1.3$ eV in the Mn–N cluster, the holes strongly hybridizing with the $3d$ electron, a considerable fraction of the $3d$ electron transfers to the hole p orbit, leading to the AFM polarization of the hole p electron with respect to the local spin. This AFM polarization is in agreement with widely observed negative As magnetic circular dichroism signal.²⁵ The strong dependence of the AFM polarization of the As or N p orbit on the hybridization strength is also shown in Fig. 1. The maximum of the polarized magnetic moment of each As(N) is about $-0.63\mu_B$ in the Mn–As cluster or $-0.32\mu_B$ in the Mn–N cluster. Our result for the Mn–N cluster is in good agreement with that obtained by the first-principles electronic structure calculation in Ref. 26 for the Mn–N clusters, but considerably larger than that obtained for periodic systems,²⁷ which is attributed to the finite size effect in Ref. 26 and the present study. Owing to four coordinates of each Mn atom, it is more reasonable to average the polarized moment on four As(N) sites, giving rise to $-0.16\mu_B$ for GaAs:Mn and $-0.08\mu_B$ for GaN:Mn. The data is in agreement with the first-principles results.²⁷

We also find that the dependence of the magnetic moment and the polarization of the p orbitals on the $3d$ energy level E_d is very similar to that on the hybridization V_{pd} in Fig. 1. For the very deep $3d$ energy level E_d , the electron in the p orbitals is weakly and positively polarized; there also exists a critical value E_c for E_d that when E_d is shallower than E_c , the electrons in the p orbitals are AFM polarized, and the polarization of the p orbit is about -40% for GaAs:Mn or -20% for GaN:Mn. One finds that the closer the E_d is to E_v , the larger the p – d hybridization is, and the more the d electrons transfer to the p orbit, hence, a stronger polarization of the p electron. A too deep or too shallow E_d level is not favorable of the formation of the AFM Mn–As(N) cluster. In the GS and for $V_{pd} = 1.0$ eV, the energy difference between FM and AFM configurations of Mn–As(N) cluster is -0.93 eV for GaAs:Mn and -1.26 eV for GaN:Mn. Obviously such a strong pd exchange energy, much larger than the hole bandwidth, invalidates the RKKY model. The pd exchange energy in GaAs:Mn quantitatively agrees with the photoemission data obtained by Okabayashi *et al.*,²⁸ in which the exchange constant is evaluated to be -1.2 ± 0.2 eV by the configuration interaction (CI) cluster model. Meanwhile, we notice that their electron occupation numbers in the d and the p orbitals differ from ours. One finds that in their Mn^{2+} state, the spin-up states in Mn are fully occupied, and only the p electrons in As(N) which have spins antiparallel to the Mn spins can transfer to the Mn $3d$ orbitals. However in our model, because of the large hybridization V_{pd} and large on-site Coulomb interaction between $3d$ electrons, the $3d$ electrons tend to transfer to the partially filled p orbitals. Thus, the $3d$ electron number of Mn in GaAs is less than 5, about 4.75, which is in agreement with the result by electronic structure

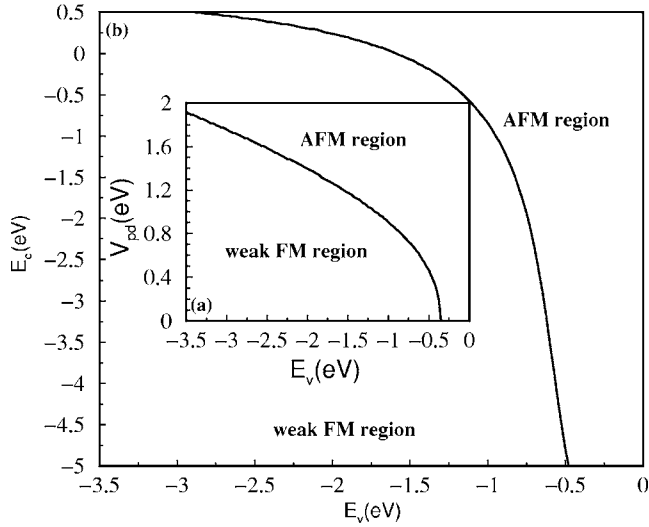


FIG. 2. The phase diagram of Mn-As(N) cluster. (a) V_{pd} vs E_v , $E_d = -0.5$ eV, and (b) E_d vs E_v , $V_{pd} = 1.0$ eV. The other parameters are the same as in Fig. 1.

calculation.²⁹ Our study also showed that the presence of the AFM polarization is not affected by the charge transfer from the d to p orbitals or from the p to d orbitals.

The magnetic phase diagrams of single Mn-As(N) cluster on E_v vs V_{pd} and V_{pd} vs E_d are shown in Figs. 2(a) and 2(b). The common character of the phase diagrams is that there exists very weak FM and strong AFM polarized regions. When both E_d and E_v are very deep, the electrons in the p orbitals are fulfilled and not polarized, this nonmagnetic region is not shown in Fig. 2. As E_d and E_v are lifted, the p electrons become weak FM polarization to the Mn spin. And for large V_{pd} and shallow E_d or E_v , the p electrons in the As(N) sites are strongly AFM polarized. Though we have little information about the exact position of the energy levels of d and p electrons in various DMS, the configuration interaction analysis in Ref. 28 showed that the realistic physical parameters of GaAs:Mn fall into the AFM region in Fig. 2. This phase diagram also provides the clue for searching new high- T_c DMS materials. The strong AFM coupling between Mn and As(N) provides such a possibility that the Mn spins interact through the AFM polarized As(N) ligands and form the FM correlation. As we showed in the following, the Mn spins establish the double-exchange-like FM coupling via the polarized p - d hybridized band. This large pd exchange coupling also validates König *et al.*'s FM spin wave theory¹⁸ for DMS, which is based on strong pd exchange interaction.

B. Magnetic coupling of two Mn spins

Next we consider two Mn-As(N) clusters to study the GS magnetic configuration and the spin couplings between Mn ions. With the increasing of Mn doping density and hole concentration, the separation between holes becomes smaller and smaller, the wave functions of these holes begin to overlap, and the holes can hop back and forth. The hopping integral between two holes at sites \mathbf{R}_i and \mathbf{R}_j is depicted by $V_h(i, j) = \langle \psi_h(\mathbf{R}_i) | h_0 | \psi_h(\mathbf{R}_j) \rangle$, where $\psi_h(\mathbf{R}_i)$ is the hole wave

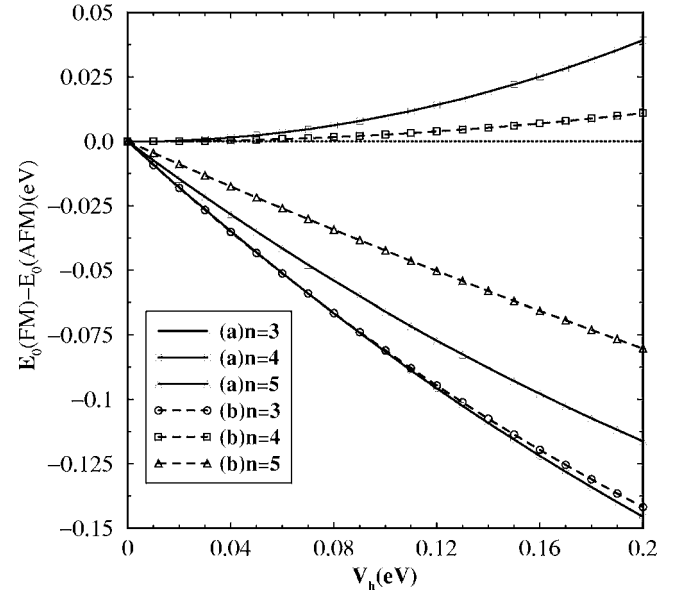


FIG. 3. Dependence of the GS energy difference between FM and AFM coupled (Mn-As) clusters on hybridization V_h , (a) GaAs:Mn and (b) GaN:Mn. $V_{pd} = 1.0$ eV, the other parameters are the same as to those in Fig. 1.

function and h_0 is the single-particle Hamiltonian. We approximate ψ_h with the hydrogen-like wave function with radius r_s and effective mass m^* , so both r_s and m^* are the functions of the Mn concentration. In this situation, the two Mn clusters interact through the hopping of holes in the two As(N) p orbitals. The summation of the lattice in Eqs. (1)–(3) runs over indices 1 and 2. For simplification, the core spins of two Mn ions are assumed semiclassical and the angle of the spins \mathbf{S}_1 and \mathbf{S}_2 is θ .

In the GS of two Mn-As clusters, the Mn local spins are either strong FM or weak AFM coupling, depending on the electron filling of the p orbitals, as shown in Fig. 3. Denote n as the total electron number of the hybridized two p and two d orbitals. Since two hybridized d orbitals are half-filling due to strong Hund's coupling and Coulomb interaction, thus $n=3$ corresponds to the electron configuration with three holes in the two p orbitals, i.e., the hole rich case; $n=4$ to that with two holes in the two p -orbitals, i.e., the half-filling case; and $n=5$ to that with a hole in the two p -orbitals, i.e., the hole poor or the hole compensation case. Comparing the GS energy of the two Mn clusters of the FM configuration with that of the AFM configuration, we find that the Mn-Mn AFM configuration is stable for the half-filled p orbitals in the two As(N) sites. However, FM configuration is more stable when the electron occupation in the As or N p orbit deviates from half-filling; and the higher the hole number is, the stronger the Mn-Mn FM coupling is. The magnetic coupling strength between two Mn spins monotonically increases with the hopping integral V_h , and the AFM coupling strength is much less than the FM coupling strength, which can be clearly seen in Fig. 3.

The microscopic origin of the magnetic couplings between Mn spins for these electron configurations can be easily understood. With the substitution doping of Mn to Ga, the local spins and holes are introduced simultaneously in the

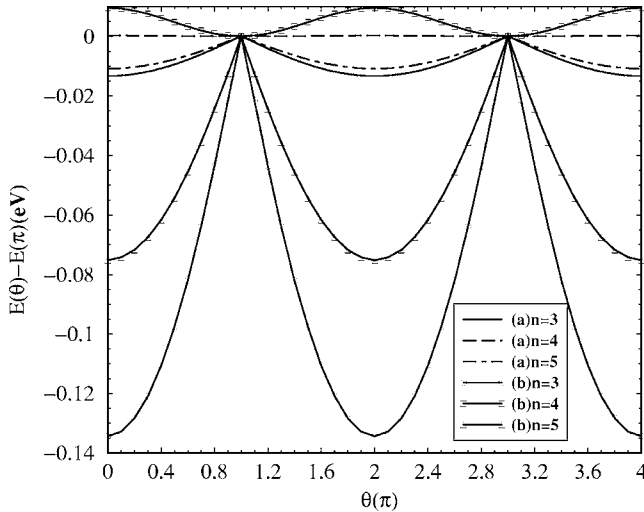


FIG. 4. The θ dependence of GS energy difference in two (Mn–As) complexes for (a) GaAs:Mn, $V_h \approx 0.015$ eV and (b) GaN:Mn, $V_h \approx 0.186$ eV. The other parameters are the same as in Fig. 3.

semiconductor host. Formally, the density of Mn spins equals to the hole concentration, it seems that the active p orbitals are always half-filled. In this situation, it is well known that the two holes interact through the AFM superexchange coupling, giving rise to the opposite spin alignment of the two p electrons. Considering the AFM coupled p - d hybridization and the strong Hund's coupling between the hybridized $3d$ electron and the local spin, one expects the AFM GS of the two Mn–As(N) clusters. On the other hand, due to the existence of numerous antisite As and the intersite Mn defects in realistic DMS, a significant fraction of holes are compensated by the electrons from these defects. Hence, the hole density in DMS is considerably less than the Mn density, and the $n=5$ electron configuration in the two Mn–As(N) clusters is the most probable in realistic DMS. As shown in Fig. 3, in the GS with hole configuration away from half-filling, the hopping of holes and their AFM hybridization with the $3d$ electrons lead to the FM coupling between Mn spins, hence to the FM GS, just as the experimental observation in GaAs:Mn, GaN:Mn, and many other DMS.

To further understand the nature of the FMLRO in DMS, we studied the dependence of the GS total energy of the two Mn–As clusters on the azimuthal angle θ between two local spins for various electron filling, and the result is shown in Fig. 4. The total energies $E(\theta)$ are measured relative to that of the Mn–Mn AFM configuration. We notice that in the half-filling p orbitals case, the energy difference $\sim \cos \theta$, indicating that the Mn–Mn coupling is the Heisenberg-like AFM. In contrast, for the case of deviating from half-filling, the GS energy difference is proportional to $|\cos \theta/2|$, and this is the essential character of the double-exchange FM in doped manganites, implying that the Mn–Mn FM coupling is double-exchange-like. Meanwhile, numerical fitting to these curves exactly gives rise to the Mn–Mn spin coupling

$$E - E_0 = J_h \cos(\theta) \sim \mathbf{S}_1 \cdot \mathbf{S}_2 \quad (4)$$

for half-filling p orbitals with $n=4$, which is the Heisenberg AFM coupling with $J_h=5.2$ meV in GaN:Mn or 0.4 meV in GaAs:Mn. In contrast, it gives rise to

$$E - E_0 \approx -J_{de} \left| \cos\left(\frac{\theta}{2}\right) \right| \sim -\sqrt{1 + \frac{\mathbf{S}_1 \cdot \mathbf{S}_2}{S^2}} \quad (5)$$

for the p orbitals configurations deviating from half-filling, and this agrees with the well-known double-exchange FM coupling in the limit of large J_H .³⁰ In the case with $n=5$, $J_{de} = 11$ meV in GaAs:Mn and $J_{de} = 75$ meV in GaN:Mn. In fact, in the present scenario that p holes strongly hybridize with the $3d$ electrons and the $3d$ electrons strongly interact with the local spins via the Hund's coupling, the $3d$ electrons form a narrow itinerant and spin-polarized band via the p holes, so that the physical interaction of Mn spins in proper doping DMS quite resembles the double-exchange interaction in doped manganites.

Experimentally, the existence of the neutral substitutional impurity state A^0 was addressed by infrared spectroscopy³¹ and the negatively ionized A^- state³² by electron paramagnetic resonance in DMS, providing the background for the double-exchange mechanism. The FM coupling energy of two Mn spins in GaAs:Mn is about 11 meV, which is comparable with the experimental Curie temperature $T_c \sim 110$ K. In GaN:Mn, the FM coupling energy is about 75 meV. Therefore, it is plausible for interpreting the origin of extremely high Curie temperature $T_c \approx 600$ – 900 K in wide-gap GaN:Mn. In comparison with the first-principles calculation for GaAs:Mn,^{23,24} the FM state is about 0.12 eV or more lower than the AFM state, much larger than what we obtained for GaAs:Mn. Such a huge difference is attributed to large unit cell and the self-consistent mean-field result in the first-principles calculation.

IV. REMARKS AND CONCLUSIONS

We find that in the AFM polarized Mn–As and Mn–N clusters, the polarized magnetic moment at the As site is larger than that at the N site both for single cluster and for two interacting clusters; on the contrary, the FM coupling energy of the Mn spins in GaAs:Mn is smaller than that in GaN:Mn. This difference arises because the charge transfer of the spin-up $3d$ electron to the p orbit in Mn–As clusters is less than that in Mn–N clusters; however, the large hopping integral of the holes in the Mn–N clusters leads to a wider hybridized band in GaN:Mn and contributes a stronger double-exchange FM coupling strength. For the systems with fulfilled p orbitals, the Mn–Mn spin coupling is the superexchange AFM, such as in Fe-doped GaAs, which is in agreement with recent first-principles result by Mahadevan and Zunger.³³ For the systems with half-filled p orbitals, different from Ref. 33 and many other first-principles results, we also predict AFM superexchange coupling between Mn spins, while the first-principles calculations predicted FM coupling. This can be addressed from two aspects: first, the $4s$ electrons of As sites are also involved to the hybridization in the first-principles calculation; second, the first-principles calcu-

lation concerns a lattice, while we consider few finite clusters. Thus on average, the p orbitals in As(N) sites are not half-filled in the first-principles calculations.

In the presence of the antisite As(N) or interstitial Mn atoms, a significant fraction of holes is compensated by the electrons from the antisite As(N) or interstitial Mn, hence the hole occupation n^c is away from half-filling, which leads to the stable double-exchange-like FM phase in realistic DMS. From Figs. 3 and 4, one finds that at n^c away from half-filling, the higher the hole number is, the stronger the Mn–Mn magnetic coupling is, and indicating a higher FM Curie temperature in DMS. Another possibility to stabilize the double-exchange-like FM phase is the inhomogeneous distribution of the hole density, such as the electronic phase separation. Since even in the molecular-beam-epitaxy-grown DMS, thin films of inhomogeneous strain were found to widely exist in most of DMS samples; this reason is in favor of the inhomogeneous distribution of the holes. With the coexistence of both configurations $n=3$ and $n=5$ in the Mn–As(N) clusters, we anticipate in the compounds with inhomogeneous hole distribution, the FM Curie temperature T_c is higher than that of the compensated compounds.

As we mentioned above, the Mn local spins in DMS are so distant in comparison with the dense spins in doped manganites that one may question the role of the double-exchange mechanism in DMS. The microscopic mechanism for the double-exchange FM coupling in Mn-doped DMS is depicted as follows: due to the strong hybridization of the As(N) p orbitals with the $3d$ electrons, the system forms two hybridized narrow bands, and the hybridized band with dominant d orbital character couples to the Mn local spins via strong Hund's coupling. Thus, the hopping of the mobile holes between localized spins gives rise to the double-exchange-like FM coupling and leads to the FM order in DMS, similar to that in doped manganites. It is worthy of stressing that the present double-exchange-like FM GS is still stable with the variation of the Mn concentration in DMS. It not only works for the present finite clusters in the high Mn concentration in the heavy doping regime, but also holds in the low doping regime. Since in low doping $\text{Ga}_{1-x}\text{Mn}_x\text{As}$ or $\text{Ga}_{1-x}\text{Mn}_x\text{N}$ thin films, as we addressed in Sec. III B, the holes form a coherent and polarized narrow band with the bandwidth of $2zV_h$, in which the hopping integral V_h depends on the hole density, i.e., the Mn concentration in DMS. Here z is the coordinate number of Mn spins. The polarized hole band hybridizes the $3d$ electrons and couples to the local spins, giving rise to the double-exchange magnetic couplings, very similar to the situation in doped manganites. Thus, the present results for finite interacting clusters can be generalized to the low Mn concentration $\text{Ga}_{1-x}\text{Mn}_x\text{As}$ or $\text{Ga}_{1-x}\text{Mn}_x\text{N}$ thin films. On the other hand, in

the limit of extremely low Mn concentration x , V_h is very small, and the hole states may be nearly compensated; therefore, the superexchange AFM coupling between Mn spins is dominant. Consequently, the GS is the AFM state or the spin-glass-like local-moment disordered state.³

Comparing the present double-exchange FM theory with the conventional double-exchange FM in manganites, we find that the valence fluctuation in the FM ordered DMS is much less than that in doped manganites. Due to the strong p - d hybridization and the extended wave functions of the p holes, the average time of the mobile electrons staying around Mn spins are nearly the same; therefore, one would not expect strong valence fluctuation in the $3d$ orbit of DMS. Meanwhile, the Curie temperature in DMS seems to be too high in comparison with the FM critical temperature in manganites, which may be attributed to the fact that the strong Jahn-Teller electron-phonon coupling and polaronic effect weakens the FM Curie point in manganites. A recent experiment by Hirakawa *et al.*¹⁰ on the infrared absorption spectroscopy in $\text{Ga}_{1-x}\text{Mn}_x\text{As}$ showed that there is no Drude peak at $\omega \rightarrow 0$, which is the characteristic of the double-exchange type of interaction observed in doped manganites, strongly supporting the double-exchange FM mechanism in FM DMS.

Obviously, the prerequisite condition for the double-exchange process is the coexistence of two kinds of Mn acceptors, the neutral impurity state A^0 with the configuration $3d^5+h$ and the ionized state A^- with $3d^5$. As we argued in the preceding, due to small valence fluctuation, the coexistence of A^- and A^0 is not easily observed in DMS. The early electron paramagnetic resonance result showed that Mn_{Ga} is in the $3d^5$ ionized state³² in $\text{Ga}_{1-x}\text{Mn}_x\text{As}$, and only the very recent resonant x-ray emission experiment³⁴ clearly demonstrated the coexistence of the two kinds of Mn acceptors, providing a direct and evident support for the important role of the double-exchange process.

In summary, we have shown that in doped III-V semiconductors, Mn–As(N) is AFM polarized only for strong p - d hybridization and small charge transfer energy. By varying the azimuthal angle between two Mn spins, we have shown that the Mn–Mn spin interaction is double-exchange-like ferromagnetic coupling, addressing the strong ferromagnetism in diluted magnetic III-V semiconductors.

ACKNOWLEDGMENTS

The authors appreciate the useful discussions with X. G. Gong, J. L. Wang, and Q.-Q. Zheng. This work was supported by the NSF of China, the BaiRen Project, and Grant No. KJCX2-SW-W11 of the Chinese Academy of Sciences (CAS). Part of the numerical calculation was performed in CCS, HFCAS.

- ¹H. Ohno, D. Chiba, F. Matsukura, T. Omiya, E. Abe, T. Dietl, Y. Ohno, and K. Ohtani, *Nature (London)* **408**, 944 (2000); F. Matsukura, H. Ohno, and T. Dietl, *Handbook of Magnetic Materials* (Elsevier, Amsterdam, 2002), Vol. 14, pp. 1–87.
- ²M. J. Seong, S. H. Chun, H. M. Cheong, N. Samarth, and A. Mascarenhas, *Phys. Rev. B* **66**, 033202 (2002).
- ³H. Akai, *Phys. Rev. Lett.* **81**, 3002 (1998).
- ⁴J. Okabayashi, T. Mizokawa, D. D. Sarma, A. Fujimori, T. Slupinski, A. Oiwa, and H. Munekata, *Phys. Rev. B* **65**, 161203(R) (2002).
- ⁵P. Kacman, *Semicond. Sci. Technol.* **16**, R25 (2001).
- ⁶H. Ohno, *Science* **281**, 951 (1998).
- ⁷H. Ohno, A. Shen, F. Matsukura, A. Oiwa, A. Endo, S. Katsumoto, and Y. Iye, *Appl. Phys. Lett.* **69**, 363 (1996).
- ⁸T. Dietl, H. Ohno, and F. Matsukura, *Phys. Rev. B* **63**, 195205 (2001).
- ⁹F. Matsukura, H. Ohno, A. Shen, and Y. Sugawara, *Phys. Rev. B* **57**, R2037 (1998).
- ¹⁰K. Hirakawa, S. Katsumoto, T. Hayashi, Y. Hashimoto, and Y. Iye, *Phys. Rev. B* **65**, 193312 (2002).
- ¹¹P. M. Krstajić, F. M. Peeters, V. A. Ivanov, V. Fleurov, and K. Kikoin, *Phys. Rev. B* **70**, 195215 (2004).
- ¹²A. Kaminski and S. Das Sarma, *Phys. Rev. Lett.* **88**, 247202 (2002).
- ¹³H. Ohno, *J. Magn. Magn. Mater.* **200**, 110 (1999).
- ¹⁴J. Okabayashi, A. Kimura, O. Rader, T. Mizokawa, A. Fujimori, T. Hayashi, and M. Tanaka, *Phys. Rev. B* **64**, 125304 (2001).
- ¹⁵E. J. Singley, R. Kawakami, D. D. Awschalom, and D. N. Basov, *Phys. Rev. Lett.* **89**, 097203 (2002).
- ¹⁶H. Åsklund, L. Ilver, J. Kanski, J. Sadowski, and R. Mathieu, *Phys. Rev. B* **66**, 115319 (2002).
- ¹⁷D. J. Priour, Jr., E. H. Hwang, and S. Das Sarma, *Phys. Rev. Lett.* **92**, 117201 (2004).
- ¹⁸J. König, H. H. Lin, and A. H. MacDonald, *Phys. Rev. Lett.* **84**, 5628 (2000).
- ¹⁹W. Nolting, T. Hickel, A. Ramakanth, G. G. Reddy, and M. Lipowczan, *Phys. Rev. B* **70**, 075207 (2004).
- ²⁰A. Zunger, in *Solid State Physics*, edited by F. Seitz, H. Ehrenreich, and D. Turnbull (Academic Press, New York, 1986), Vol. 39, p. 275.
- ²¹A. Zunger and U. Lindefelt, *Phys. Rev. B* **27**, 1191 (1983).
- ²²C. Delerue, M. Lannoo, and G. Allan, *Phys. Rev. B* **39**, 1669 (1989).
- ²³S. Sanvito, P. Ordejón, and N. A. Hill, *Phys. Rev. B* **63**, 165206 (2001).
- ²⁴Yu-Jun Zhao, W. T. Geng, K. T. Park, and A. J. Freeman, *Phys. Rev. B* **64**, 035207 (2001).
- ²⁵B. Beschoten, P. A. Crowell, I. Malajovich, D. D. Awschalom, F. Matsukura, A. Shen, and H. Ohno, *Phys. Rev. Lett.* **83**, 3073 (1999).
- ²⁶B. K. Rao and P. Jena, *Phys. Rev. Lett.* **89**, 185504 (2002).
- ²⁷Shi-hao Wei, X. G. Gong, G. M. Dalpian, and Su-huai Wei (unpublished).
- ²⁸J. Okabayashi, A. Kimura, O. Rader, T. Mizokawa, A. Fujimori, T. Hayashi, and M. Tanaka, *Phys. Rev. B* **58**, R4211 (1998).
- ²⁹E. Kulatov, H. Nakayama, H. Mariette, H. Ohta, and Yu. A. Usenskii, *Phys. Rev. B* **66**, 045203 (2002).
- ³⁰P. W. Anderson and M. Hill, *Phys. Rev.* **100**, 675 (1955).
- ³¹M. Linnarsson, E. Janzén, B. Monemar, M. Kleverman, and A. Thilderkvist, *Phys. Rev. B* **55**, 6938 (1997).
- ³²J. Szczytko, A. Twardowski, K. Swiatek, M. Palczewska, M. Tanaka, T. Hayashi, and K. Ando, *Phys. Rev. B* **60**, 8304 (1999).
- ³³P. Mahadevan and A. Zunger, *Phys. Rev. B* **69**, 115211 (2004).
- ³⁴Y. Ishiwata, T. Takeuchi, R. Eguchi, M. Watanabe, Y. Harada, K. Kanai, A. Chainani, M. Taguchi, S. Shin, M. C. Debnath, I. Souma, Y. Oka, T. Hayashi, Y. Hashimoto, S. Katsumoto, and Y. Iye, *Phys. Rev. B* **71**, 121202(R) (2005).